Acknowledgments. We thank the National Institutes of Health (GM 15166) and the National Science Foundation (GP 14607) for support of this work. Preliminary investigations were carried out by Mr. G. A. Segal, a National Science Foundation undergraduate research participant, summer 1967.

Solvent Steric Effects. III. Molecular and Crystal Structures of Azobisisobutyronitrile and Azobis-3-cyano-3-pentane. A Structural Deuterium Isotope Effect[1]

Annette B. Jaffe,[2a] Donald S. Malament,[2b] Edwin P. Slisz, and J. Michael McBride*[2c]

Contribution from the Department of Chemistry, Yale University, New Haven, Connecticut 06520. *Received December 2, 1971*

Abstract: Lattice parameters were determined for normal and perdeuterated azobisisobutyronitrile (AIBN) in $P\bar{1}$ and $P2_1/c$ modifications and showed significant variation with isotopic substitution. Three dimensional intensity data were collected by diffractometer for three of these crystals and for a crystal of azobis-3-cyano-3-pentane (ACP) and all were refined to conventional R's of 0.05–0.09. The refinement of ACP was in space group $Cmca$ ($Z = 4$) and gave a long C–C bond, a wide C–C–C angle, and unrealistic thermal parameters suggesting disorder with respect to the mirror plane which was confirmed by the observation of diffuse scattering. Otherwise bond lengths and angles are consistent among the determinations and with those of other azoalkanes. The nitrile and azo groups are nearly eclipsed to give planar, S-shaped N≡CCN=NCC≡N backbones for molecules in these crystals. The backbones are arranged into sheets containing a herringbone pattern of nitrile groups. The photochemistry of crystalline AIBN and ACP is discussed in terms of these packings, and it is concluded that dipolar forces are probably predominant in product determination. An approach to computer simulation of radical reactions in crystalline matrices is mentioned. The thermal transformation of $P2_1/c$ AIBN to $P\bar{1}$ AIBN is not consistently topotactic.

Azobisisobutyronitrile (AIBN) crystallizes from methanol in two modifications.[1a] Photolysis of either generates pairs of cyanoisopropyl radicals which collapse to give abnormally high yields of the disproportionation products isobutyronitrile (IBN) and methacrylonitrile (MAN), low yields of the symmetrical coupling product tetramethylsuccinodinitrile (TMSN), and little or none of the unsymmetrical coupling product dimethyl-*N*-(2-cyano-2-propyl)ketenimine (KI), which predominates in the solution reaction.[1a] To interpret this reactivity pattern and to analyze the epr spectrum of the metastable intermediate triplet-state radical pairs[3] it is necessary to know the geometry of the lattice in which reaction occurs.

Since we have studied deuterated as well as unlabeled AIBN in our other work, we decided to investigate isotope effects on the crystal structures in addition to determining the crystal structures themselves. Such isotope effect studies of organic molecules seem previously to have been confined to methane[4] and certain hydrogen bonded systems.[5]

The solution photochemistry of azobis-3-cyano-3-pentane (ACP), the analog of AIBN in which methyl groups are replaced by ethyl, is quite similar to that of AIBN. However in contrast to AIBN, solid-state photolysis of ACP yields a product distribution similar to that found in solution, giving substantial amounts of tetraethylsuccinodinitrile and ketenimine and negligible amounts of disproportionation products.[1a] We also undertook the determination of an approximate molecular structure and crystal packing for disordered crystals of this compound.

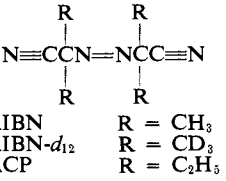

The success of others in using empirical atom–atom potentials to calculate crystal packing energies[6] suggested the possibility of simulating reaction paths in the crystalline environment of AIBN by analogous calculations. For these calculations a set of realistic values of the pairwise potentials must be available, and at the end of this paper we touch on some first steps toward defining such a set of potentials for our system.

Experimental Section

AIBN. AIBN crystals grown from methanol solution at room temperature[1a,7] were mounted among red cotton fibers in 0.5-mm

(1) (a) Part II: A. B. Jaffe, K. J. Skinner, and J. M. McBride, *J. Amer. Chem. Soc.*, **94**, 8510 (1972); (b) presented in part at the 158th National Meeting of the American Chemical Society, New York, N. Y., Sept 1969, Abstract ORGN-118, and at the Second International Symposium on Organic Solid-State Chemistry, Rehovot, Sept 1970, Abstract Ic.

(2) (a) NASA Trainee, 1969–1970; (b) National Institutes of Health Predoctoral Fellow, 1966–1969; (c) Alfred P. Sloan Foundation Fellow.

(3) (a) Ya. S. Lebedev, *Dokl. Akad. Nauk SSSR*, **171**, 378 (1966); (b) A. B. Jaffe and J. M. McBride, to be submitted for publication.

(4) S. C. Greer and L. Meyer, *J. Chem. Phys.*, **52**, 468 (1970).

(5) K. J. Gallagher, "Hydrogen Bonding," D. Hadzi, Ed., Pergamon Press, New York, N. Y., 1959, p 45.

(6) See for example, (a) D. E. Williams, *J. Chem. Phys.*, **45**, 3770 (1966); **47**, 460 (1967); (b) E. Giglio and A. M. Liquori, *Acta Crystallogr.*, **22**, 437 (1967); (c) A. I. Kitaigorodskii, *ibid.*, **18**, 585 (1965); (d) R. Mason, *Mol. Cryst. Liquid Cryst.*, **9**, 1 (1969).

Table I. AIBN Lattice Parameters[a]

	$C_8H_{12}N_4$, mol wt 164.21	$C_8D_{12}N_4$, mol wt 176.28	Difference
	Triclinic,[b] $P\bar{1}$, $Z = 1$		
a	7.865(2)	7.855(2, 3)	0.010
b	5.555(1)	5.549(1, 1)	0.006
c	6.201(1)	6.204(1, 1)	−0.003
α	71.33(1)	71.31(1, 0)	0.02
β	77.95(2)	77.98(2, 2)	−0.03
γ	79.19(2)	79.25(2, 1)	−0.06
Vol	248.9	248.4	0.5
ρ_c	1.096	1.178	
	Monoclinic,[c] $P2_1/c$, $Z = 2$		
a	5.509(1, 2)	5.501(1, 2)	0.008
b	8.225(2, 1)	8.219(2, 3)	0.006
c	11.002(2, 1)	10.989(3, 6)	0.013
β	96.00(1, 1)	95.98(2, 2)	0.02
Vol	495.8	494.1	1.7
ρ_c	1.100	1.185	

[a] Estimated standard deviations in the final digit as determined during least-squares refinement are given in parentheses. When two figures are given, the parameter is the average of two determinations, the first figure in parentheses is the larger estimated deviation in the final digit, and the second is the deviation of the experimental values from their average. [b] This unit cell was chosen for convenience since the reduced cell has one very large angle which complicates refinement. The reduced cell has $a = 6.874$ Å, $b = 7.865$ Å, $c = 8.942$ Å, $\alpha = 92.11°$, $\beta = 114.45°$, and $\gamma = 137.30°$ and may be derived from the reported cell by the transformation $0\bar{1}1/\bar{1}00/10\bar{1}$. [c] A previous study (ref 15) on unlabeled monoclinic crystals grown from chloroform–petroleum ether gave $a = 5.506$ (4) Å, $b = 8.236$ (8) Å, $c = 10.995$ (8) Å, and $\beta = 96.07$ (4)°.

quartz capillaries sealed with wax. Space groups for the two modifications were determined from Weissenberg and precession photographs, which showed the predicted absences ($P\bar{1}$, none; $P2_1/c$, $h0l$ for l odd, $0k0$ for k odd). Centrosymmetry of the triclinic crystal was confirmed during structure refinement. Quantitative measurements were made at room temperature[8] with a Picker FACS-1 diffractometer system with pulse-height analysis and Mo Kα radiation isolated by a graphite monochromator. In each case lattice parameters (see Table I) were refined by least squares[9] using 12 carefully centered reflections of $36° < 2\theta < 43°$ with averaging of positive and negative 2θ angles for Kα_1 (0.70926 Å). In three of the four cases accurate lattice parameters of new crystals were redetermined by the same method after a 1-year interval. The consistency of these determinations is indicated in Table I.

Intensity data were collected using ω scan as indicated in Table II. The crystals used showed no evidence of X-ray induced damage as judged by the repeated measurement of standard reflections near each of the principal axes. Background, Lorentz, and polarization corrections were applied, but absorption was ignored ($\mu < 0.71$ cm^{-1}).

Nonhydrogen atoms were located from sharpened Patterson maps and the hydrogens in subsequent difference syntheses. In the final cycles of full-matrix least-squares refinement[10] all atomic coordinates were varied as well as a scale factor, anisotropic thermal parameters for the nonhydrogen atoms, and isotropic thermal parameters for the hydrogens.[11] Table III presents standard criteria for evaluating the refinements, and Tables IV and V give the final atomic coordinates and thermal parameters with standard errors measured by the inverse matrix of refinement.

AIBN Phase Transformation. The $P\bar{1}$ pseudomorph which replaces a single $P2_1/c$ needle on heating to 70–80°[1a] is often sufficiently transparent and oriented to transmit and extinguish light when viewed between crossed polaroids. Because of the packing similarities between the two modifications we studied the transformation for possible topotaxy. Two single $P2_1/c$ needles about 0.3 mm thick were sealed in 0.5-mm quartz capillaries, and their alignment was determined by oscillation, Weissenberg, and precession photographs. Without disturbing the goniometer head the crystals were examined by polarizing microscope for signs of the phase transition during slow heating by a nearby hot wire. One crystal became cloudy before appearance of $P\bar{1}$ reflections, but both ultimately became pseudomorphs which were somewhat cloudy and cracked and gave only $P\bar{1}$ reflections. Mosaic spread was quite large in the new phase with reflections as much as 10–15° wide about the needle axis, and one of the two crystals gave a twinned daughter. Alignment of the daughter phase was determined

Table II. Data Collection

	AIBN $P\bar{1}$	AIBN-d_{12} $P\bar{1}$	AIBN $P2_1/c$	ACP $Cmca$	
Crystal size, mm	0.2 × 0.2 × 0.2	0.2 × 0.15 × 0.2	0.2 × 0.15 × 0.25	0.3 × 0.2 × 0.1	
ω spread,[a] deg	0.08	0.10	0.10	0.05	
2θ range, deg	3–55	3–54.5	3–53	2–40	40–46
ω scan speed, deg/min	0.125	0.50	0.125	0.25	0.125
ω scan range,[b] deg	0.5	1.0	0.6	0.6	
Background count, sec	80	80	80	80	
Independent reflections	1008	993	803	554	
Reflections omitted[c]	11	33	0	3	

[a] Width of low-angle peaks with narrow detector slits. [b] See ref 9 for scanning method. [c] From least-squares refinement.

Table III. Refinement Criteria

	AIBN $P\bar{1}$	AIBN-d_{12} $P\bar{1}$	AIBN $P2_1/c$
R_w[a]	0.074	0.051	0.046
R[b]	0.092	0.070	0.061
$\lvert\rho\rvert_{max}$[c]	0.22	0.14	0.12

[a] $(\Sigma w(|F_o| - |F_c|)^2/\Sigma wF_o^2)^{1/2}$ for reflections used in refinement. [b] $\Sigma||F_o| - |F_c||/\Sigma|F_o|$ for reflections used in refinement. [c] Maximum density (e/Å^3) in final difference map based on all reflections used in refinement.

(7) It seemed that AIBN-h_{12} crystallized more readily as monoclinic needles elongated along [100] and AIBN-d_{12} as triclinic plates showing (100). Occasionally at lower temperature the (011) face was highly developed for the monoclinic modification giving a plate-like crystal.

(8) No effort was made to control the temperature of the crystals during the measurement of lattice parameters (the temperature of the room was 21 ± 1.5° during the original determination of lattice parameters and 26 ± 2° when three of these sets of parameters were redetermined). Our study of the variation of the parameters with temperature down to 77°K shows that 10–20° temperature differences would be required to cause the variations observed between labeled and unlabeled samples. We thank Mr. E. T. Koh for his assistance in these measurements.

(9) See W. R. Busing, *et al.*, Report ORNL-4143, Oak Ridge National Laboratory, Oak Ridge, Tenn., 1968.

(10) W. R. Busing, K. O. Martin, and H. A. Levy, "OR XFLS3," Oak Ridge National Laboratory, Oak Ridge, Tenn., 1971. Minimizing $\Sigma w(|F_o| - |F_c|)^2$. Scattering factors for hydrogen were taken from R. F. Stewart, E. R. Davidson, and W. T. Simpson, *J. Chem. Phys.*, **42**, 3175 (1965); for carbon and nitrogen from D. T. Cromer and J. B. Mann, *Acta Crystallogr., Sect. A*, **24**, 321 (1968).

(11) All reflections were given equal weight, but some were omitted during refinement because of suspected extinction or experimental uncertainty surrounding their measurement. These are indicated by asterisks in Tables X–XIV of calculated and observed structure factors which will appear following these pages in the microfilm edition of this volume of the journal. Single copies may be obtained from the Business Operations Office, Books and Journals Division, American Chemical Society, 1155 Sixteenth St., N.W., Washington, D. C. 20036, by re-

Table IV. Fractional Atomic Coordinates for AIBN[a]

	AIBN, $P\bar{1}$			AIBN-d_{12}, $P\bar{1}$			AIBN, $P2_1/c$		
	x	y	z	x	y	z	x	y	z
N(1)	−369 (3)	−335 (4)	999 (3)	−373 (2)	−331 (3)	992 (3)	173 (4)	729 (2)	53 (2)
N(2)	−2778 (4)	5200 (6)	−2013 (5)	−2780 (3)	5209 (4)	−2017 (4)	−4687 (4)	63 (3)	−2178 (2)
C(1)	−2084 (3)	1267 (5)	1480 (4)	−2070 (3)	1264 (4)	1483 (3)	−1477 (4)	1755 (3)	−793 (2)
C(2)	−2436 (4)	3458 (6)	−535 (5)	−2434 (3)	3477 (4)	−544 (4)	−3270 (4)	771 (3)	−1569 (2)
C(3)	−3487 (4)	−484 (7)	2143 (6)	−3496 (3)	−492 (5)	2140 (5)	−2802 (7)	2909 (4)	2 (3)
C(4)	−1960 (5)	2211 (7)	3478 (6)	−1950 (4)	2202 (6)	3485 (5)	132 (5)	2678 (4)	−1599 (3)
H(1)	−472 (8)	43 (11)	272 (10)	−469 (3)	56 (4)	246 (4)	−379 (4)	367 (3)	−52 (2)
H(2)	−316 (5)	−179 (7)	353 (7)	−322 (3)	−189 (5)	351 (4)	−384 (5)	229 (3)	50 (2)
H(3)	−355 (4)	−128 (6)	98 (5)	−352 (3)	−107 (4)	82 (4)	−149 (4)	344 (3)	45 (2)
H(4)	−169 (4)	71 (6)	474 (6)	−175 (4)	72 (5)	482 (5)	−84 (4)	345 (3)	−215 (2)
H(5)	−115 (4)	343 (7)	316 (5)	−106 (3)	334 (5)	307 (4)	108 (3)	195 (2)	−204 (2)
H(6)	−299 (5)	343 (8)	389 (7)	−308 (3)	318 (4)	387 (4)	139 (4)	324 (3)	−105 (2)

[a] × 10^4 for N and C; × 10^3 for H. Estimated standard deviations in the final digit are given in parentheses.

Table V. Anisotropic Temperature Factors (×10^4)[a,b]

	β_{11}	β_{22}	β_{33}	β_{12}	β_{13}	β_{23}
			AIBN, $P\bar{1}$			
N(1)	175 (4)	383 (9)	254 (6)	77 (5)	−25 (4)	−54 (6)
N(2)	344 (8)	578 (14)	357 (10)	209 (8)	−10 (7)	0 (9)
C(1)	162 (5)	338 (9)	255 (8)	76 (5)	−34 (5)	−62 (7)
C(2)	196 (6)	434 (12)	292 (9)	103 (6)	−13 (5)	−62 (8)
C(3)	202 (6)	472 (14)	394 (12)	20 (7)	−28 (7)	−135 (10)
C(4)	244 (7)	511 (15)	342 (11)	40 (9)	−53 (7)	−173 (10)
H[b]	14.3 (20)	9.2 (10)	6.4 (7)	7.1 (8)	7.6 (8)	9.2 (11)
			AIBN-d_{12}, $P\bar{1}$			
N(1)	176 (3)	399 (7)	279 (5)	62 (4)	−36 (3)	−72 (5)
N(2)	354 (6)	559 (10)	383 (8)	167 (6)	−17 (5)	7 (7)
C(1)	178 (4)	375 (8)	255 (6)	57 (4)	−31 (4)	−47 (5)
C(2)	205 (4)	443 (9)	317 (7)	74 (5)	−15 (4)	−68 (7)
C(3)	211 (5)	456 (10)	413 (9)	28 (6)	−45 (5)	−106 (8)
C(4)	248 (6)	531 (12)	372 (9)	22 (7)	−41 (5)	−166 (8)
H[b]	6.4 (5)	7.2 (6)	5.9 (5)	7.7 (7)	6.4 (7)	5.6 (6)
			AIBN, $P2_1/c$			
N(1)	395 (7)	126 (3)	93 (2)	−5 (4)	−10 (3)	3 (2)
N(2)	460 (10)	225 (5)	138 (3)	−16 (6)	−48 (4)	−15 (3)
C(1)	353 (8)	134 (4)	86 (2)	14 (5)	−10 (3)	10 (2)
C(2)	342 (8)	158 (4)	97 (2)	14 (5)	1 (3)	7 (2)
C(3)	546 (13)	160 (5)	114 (3)	48 (7)	6 (5)	−7 (3)
C(4)	401 (10)	198 (5)	131 (3)	−10 (6)	6 (5)	43 (3)
H[b]	6.8 (6)	6.9 (6)	6.7 (5)	6.1 (6)	5.4 (4)	6.3 (5)

[a] Estimated standard deviations in the final digit are given in parentheses. Values are for temperature factor of the form $\exp[-(h^2\beta_{11} + k^2\beta_{22} + l^2\beta_{33} + 2hk\beta_{12} + 2hl\beta_{13} + 2kl\beta_{23})]$. [b] Last row in each set gives *isotropic* temperature factors (B) of the six hydrogen atoms in numerical order not multiplied by 10^4.

from overlapping 65° oscillation photographs supplemented by screenless Weissenberg photographs. The matrices which transform fractional coordinates from daughter ($P\bar{1}$) to parent ($P2_1/c$) are

$$\begin{bmatrix} -0.2516 & -0.7074 & 0.5001 \\ 0.7871 & -0.2238 & -0.1725 \\ 0.3730 & 0.2838 & 0.5151 \end{bmatrix}$$

for one crystal and

$$\begin{bmatrix} -0.0424 & 0.2516 & -0.9547 \\ 0.4343 & 0.6363 & 0.4073 \\ 0.6344 & -0.0976 & -0.0799 \end{bmatrix}$$

$$\begin{bmatrix} 0.2449 & -0.2679 & 0.9395 \\ -0.0047 & -0.6332 & -0.4224 \\ 0.7172 & 0.0968 & 0.0821 \end{bmatrix}$$

for the twins of the second crystal. The orientations of these daughters have little in common with each other or with the parent phase except that the twins share an a^* axis which is within 13° of the c^* axis of the parent crystal and the single-crystal daughter has the normal to its (111) within 22° of the c^* axis of the parent. We have found no evidence for an intermediate fluid phase, but no convincing argument for topotaxy or epitaxy is suggested by these observations.

ACP. ACP crystals were grown from methanol solution at room temperature as plates showing (001). Weissenberg and precession photographs at very long exposure showed a C-centered orthorhombic system with a pattern of systematic absences (hkl, $h + k$ odd; $h0l$, l odd; $hk0$ h odd) consistent with space group *Cmca* (64) or *C2ca* (*Aba*2, 41). These photographs also showed streaks of diffuse scattering parallel to b in ($h00$) planes with h odd.

Crystal mounting, cell constant determination, and data collection over one-fourth of the reflection sphere were as described above for AIBN (see Table II). The cell constants were the following: $C_{12}H_{20}N_4$, mol wt 220.31, orthorhombic, a = 9.059 (2) Å, b = 9.966 (1) Å, c = 15.559 (3) Å, $\alpha = \beta = \gamma$ = 90.00 (2)°, V = 1404.5 Å^3, ρ_c = 1.0418, Z = 4. During data collection three standards were monitored after each 60 reflections and the limits of the intensity variation among 20 sets of determinations were ±1.5, 2, and 3%, respectively.

Observed intensities were corrected for background, Lorentz, and polarization effects but not for absorption, since the maximum correction would be less than 2% (μ 0.618 cm^{-1}). Intensities of the strongest three reflections were augmented by 4% to correct for a coincidence error in counting indicated by remeasuring the 12 most

ferring to code number JACS-72-8515. Remit check or money order for $4.00 for photocopy or $2.00 for microfiche.

intense reflections at reduced power but were assigned zero weight in final stages of refinement because of apparent extinction. Of the 554 independent reflections including absences not due to centering within $(\sin\theta/\lambda) < 0.540$, 92 were collected at three symmetrically equivalent positions and 322 at two. After averaging equivalent reflections, 160 reflections had intensities less than 1.33 times the rms intensity of the 57 systematic absences. In the final stages of refinement these were each assigned the averaged calculated F for the group and included with one-fourth the weight of the other "observed" reflections. Consistency of the data was checked by evaluating $\Sigma||F_o| - |F_{av}||\Sigma|F_o|$ over all observations of reflections measured in more than one position. This limiting R was 0.032 over 393 nonabsent reflections and 0.013 over 248 "observed" reflections.

Results of the zero moment test of Howells, Phillips, and Rogers[12] were consistent with the centric group *Cmca* in which the four molecules in a unit cell must have $2/m$ symmetry with all atoms except the ethyl groups constrained to the mirror plane. A Patterson map suggested positions for five of the six nonhydrogen atoms in the asymmetric unit and a difference synthesis revealed the terminal carbon. A difference synthesis after preliminary refinement of this model with individual anisotropic temperature factors gave the five hydrogens as the only peaks but two of density greater than 0.16 e/Å^3 (ρ_{max} = 0.28). Refinement with isotropic temperature factors for the hydrogens and anisotropic for the other atoms gave R = 0.076, R_w = 0.044 for the fractional coordinates and thermal parameters of Tables VI and VII.

Table VI. Fractional Atomic Coordinates from Ordered Refinement of ACP[a]

Atom	x	y	z
N(1)	0[b]	0.0600 (2)	0.0076 (2)
N(2)	0[b]	−0.1117 (3)	0.2015 (2)
C(1)	0[b]	0.0963 (3)	0.1008 (2)
C(2)	0[b]	−0.0238 (3)	0.1565 (2)
C(3)	0.1402 (7)	0.1793 (4)	0.1176 (2)
C(4)	0.2832 (9)	0.1080 (7)	0.1109 (4)
H(1)	0.132 (3)	0.219 (3)	0.174 (2)
H(2)	0.129 (3)	0.259 (3)	0.077 (2)
H(3)	0.277 (5)	0.032 (3)	0.151 (2)
H(4)	0.295 (4)	0.070 (3)	0.059 (2)
H(5)	0.365 (5)	0.186 (6)	0.121 (3)

[a] Estimated standard deviations in the final digit are given in parentheses. [b] Constrained by symmetry to x = 0.

plane, attempts were made to refine the structure without hydrogen atoms in subgroups of *Cmca* which are C centered but lack the mirror ($P2_1/c$ 14, $C2/c$ 15, $C222_1$ 20, $Aba2$ 41). In each case the mirror symmetry of the model was broken by displacing the atoms by about 0.2 Å before refinement, but in no case were the thermal parameters significantly reduced by two refinement cycles. Noncentered subgroups of *Cmca* lacking the mirror plane (*Pcca* 54, *Pccn* 56, *Pbcn* 60, *Pbca* 61) were excluded by the systematic absences which were checked carefully.

Although an F_o synthesis showed no trace of resolution of disordered atoms, a ΔF synthesis showed 12 peaks of density greater than 0.1 e/Å^3 ($|\rho|_{max}$ 0.165) 11 of which could be explained in terms of disordering with respect to the mirror plane. The other peak (0.12 e/Å^3) was appropriate for the unshared electron pair on azo nitrogen. Full-matrix refinement for the disordered structure was precluded by the strong correlation between x and β_{11} for atoms near the mirror (correlation coefficients 0.87 to 0.96). In attempts to refine the disordered structure the hydrogen parameters were fixed and only observed reflections were used. Two least-squares cycles were calculated in which the ethyl carbons were each divided and the halves centered 0.225 Å along the major thermal axis from the parent ordered atoms and their thermal parameters varied, while for the mirror plane atoms x was held at $0.025a$ (0.226 Å) and all other parameters were varied. This gave R_w = 0.028. Through two more cycles x (but not β_{11}) for the mirror plane atoms and all other heavy-atom parameters were refined, and finally two cycles were calculated varying all parameters but mirror plane atom x. The final R_w was 0.026 giving an R factor ratio of 1.46 with a previous ordered refinement using the same reflections. For this "disordered" refinement there were 245 degrees of freedom and 30 more parameters than for the "ordered" so that a ratio of 1.12 would be deemed significant at the 99.9% confidence level.[13,14] The largest peak in a difference map on this model using all nonextinguished reflections was 0.155 e/Å^3 and was positioned appropriately (0, −0.120, 0.0264) to represent the unshared electron pair of the azo nitrogen. All other peaks were less than 0.11 e Å^3; the largest of these were around the nitrile carbon and between the side chain carbons.

The thermal ellipsoids of atoms near the mirror plane were much more reasonable for this "disordered" model, the largest rms displacement being 0.36 Å. However ellipsoids for the ethyl carbons were as bad as they had been previously and bond lengths and angles gave much poorer agreement with those of AIBN.

Discussion

Molecular Geometry. AIBN. The molecular geometry and atomic numbering scheme are shown in Figure 1 for triclinic AIBN. The numbering scheme for the monoclinic form is the same and the geometry is nearly identical. The bond lengths and angles

Table VII. Temperature Factors[a] (×10^4) from Ordered Refinement of ACP

Atom	β_{11}	β_{22}	β_{33}	β_{12}	β_{13}	β_{23}
N(1)	397 (8)	104 (3)	34 (1)	0[b]	0[b]	−2 (2)
	0.41	0.23	0.20			
N(2)	490 (11)	177 (4)	47 (1)	0[b]	0[b]	18 (2)
	0.45	0.31	0.23			
C(1)	411 (11)	109 (4)	33 (1)	0[b]	0[b]	−5 (2)
	0.41	0.24	0.20			
C(2)	331 (9)	147 (5)	34 (1)	0[b]	0[b]	−8 (2)
	0.37	0.27	0.20			
C(3)	608 (14)	175 (5)	55 (2)	−117 (7)	8 (4)	−24 (2)
	0.52	0.29	0.23			
C(4)	496 (15)	381 (12)	101 (3)	−177 (12)	29 (6)	−60 (5)
	0.54	0.37	0.31			
H[c]	11.1 (8)	12.9 (10)	14.5 (16)	12.3 (11)	30.0 (29)	
	0.37	0.40	0.43	0.39	0.62	

[a] Estimated standard deviations in the final digit are given in parentheses. The second row for each atom gives the root-mean-square thermal amplitude (Å) along the principle axes of the diagonalized tensor. For the first four entries the largest displacement is normal to the mirror plane; for the fifth it is very close to this direction. Values are for temperature factor of the form $\exp[-(h^2\beta_{11} + k^2\beta_{22} + l^2\beta_{33} + 2hk\beta_{12} + 2hl\beta_{13} + 2kl\beta_{23})]$. [b] Constrained to zero by symmetry. [c] Isotropic temperature factors (B) of the five hydrogen atoms in numerical order not multiplied by 10^4. The second row gives the rms thermal amplitude in Å.

For the most part the bond lengths and angles are reasonable (Table VIII), but the large thermal parameters suggested disorder. Since for atoms on the mirror plane the major axis is normal to the

(12) E. R. Howells, D. C. Phillips, and D. Rogers, *Acta Crystallogr.*, 3, 210 (1950).

(13) W. C. Hamilton, *Acta Crystallogr.*, **18**, 502 (1965).

(14) G. S. Pawley, *Acta Crystallogr., Sect. A*, 26, 691 (1970).

Table VIII. Molecular Geometries of Some Azoalkanes[a]

	AIBN $P\bar{1}$	AIBN-d_{12} $P\bar{1}$	AIBN $P2_1/c$	ACP[b] $Cmca$	CPAP[c] $P\bar{1}$	APP[d] $C2/c$ 2	APP[d] $C2/c$ $\bar{1}$
			Bond Lengths, Å				
N=N	1.223 (4)	1.218 (3)	1.217 (3)	1.218 (4)	1.24	1.220 (4)	1.233 (4)
=N—C	1.501 (3)	1.488 (2)	1.492 (3)	1.496 (4)	1.47	1.493 (4)	1.499 (3)
C≡N	1.134 (3)	1.130 (3)	1.135 (2)	1.122 (4)			
C—C≡	1.471 (3)	1.483 (3)	1.477 (3)	1.477 (5)			
C—CH_2	1.513 (4)	1.518 (3)	1.522 (3)	1.538 (5)	1.56	1.535 (5)	1.532 (4)
	1.518 (4)	1.527 (3)	1.524 (3)	1.481 (8)[e]	1.57	1.535 (4)	1.547 (4)
C—H	0.82–1.07	0.97–1.03	0.95–0.99	0.90–1.08			
			Bond Angles, Deg				
N=N—C	114.2 (2)	114.8 (2)	114.8 (2)	115.2 (3)	116	113.5 (3)	114.3 (3)
=N—C—C≡	111.9 (2)	112.0 (2)	112.0 (2)	111.9 (3)			
C—C≡N	176.3 (3)	176.5 (2)	177.5 (2)	177.2 (3)			
=N—C—CH_2	106.6 (2)	106.6 (2)	106.9 (2)	107.2 (2)	107	105.1 (2)	103.7 (2)
	106.6 (2)	107.1 (2)	106.9 (2)		108	112.8 (2)	114.1 (2)
≡C—C—CH_2	110.5 (2)	110.2 (2)	109.4 (2)	109.7 (2)			
	110.0 (2)	109.9 (2)	109.9 (2)				
H—C—H	104–112	107–114	103–114	104–112			
			Torsional Angle, Deg				
N=N—C—C≡N	−4.9 (4)	−4.3 (3)	1.9 (3)	0[f]	0, 16[g]	154.8[h]	98.6 (2)[h]
N=N—C—CH_2	116.0 (3)	115.9 (3)	122.3 (3)	120.2 (3)		33.2	−16.3 (1)
	−125.3 (3)	−125.2 (3)	−118.0 (3)			−86.2	−138.4 (3)
=N—C—C≡N	160 (5)	170 (5)	173 (6)	180 (0[f])			

[a] Esd of final digit given in parentheses. [b] The molecular parameters of ACP are not definitive, since the crystal is disordered and gives abnormally high thermal parameters for this refinement in *Cmca*. [c] 1,1′-Dichloro-1,1′-diphenyl-1,1′-azopropane, ref 16. [d] Two crystallographically independent molecules of azobis-3-phenyl-3-pentane. See K. J. Skinner, R. J. Blaskiewicz, and J. M. McBride, *Isr. J. Chem.*, **10**, 457 (1972). [e] C(3)–C(4) bond distance. [f] Fixed by space group symmetry. [g] Cl for C≡N in formula. [h] Phenyl for C≡N in formula.

for the three structures reported here are unexceptional and show good consistency from one determination to the next. They are presented in Table VIII together with analogous data for ACP and two other azoalkanes. Recently Argay and Sasvári have reported an independent determination of the structure of the $P2_1/c$ modification based on 1023 reflections collected photographically and refined to $R = 0.11$.[15] All of their atomic coordinates agree with ours within two standard deviations for the heavy atoms and three standard deviations for the hydrogens. The bond lengths and angles are in similar agreement.

Table VIII shows torsional angles about the azo-carbon bonds. The nitrile groups in both AIBN modifications as well as in ACP are nearly eclipsed with the azo nitrogen, occupying positions analogous to those assumed by chlorine in 1,1′-dichloro-1,1′-diphenyl-1,1′-azopropane.[16] This conformation is of considerable chemical interest, because it might have been thought *a priori* to have been the most likely conformation for yielding KI on photolysis, whereas in fact this product is not observed for AIBN. Because of the eclipsed conformation the molecules are most easily visualized as nearly planar S-shaped N≡CCN=NCC≡N backbones with alkyl groups above and below the plane. Argay and Sasvári noted that the molecule's deviation from noncrystallographic $2/m$ symmetry is barely within the limits of experimental error for the $P2_1/c$ modification. Examination of the torsional angles about the C(1)–N(1) bond shows that departure from $2/m$ symmetry is experimentally significant for both modifications.

A minor but consistent conformational detail is the nonlinearity of the C—C≡N nitrile grouping by as much as 3.7°. The =NCC≡N torsional angles show that, as in the determination of Argay and Sasvári, the nitrile nitrogen is bent away from the azo nitrogens.

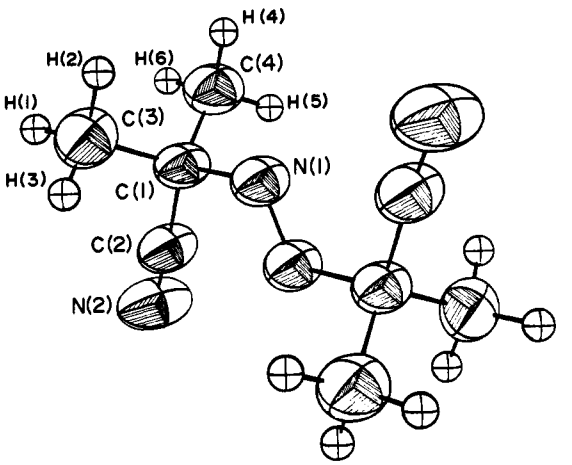

Figure 1. Molecular structure of AIBN-d_{12} in $P\bar{1}$ modification viewed along increasing b^* with the a axis horizontal and x increasing to the right. The far half of the molecule is numbered as in Table IV, and thermal ellipsoids are drawn at the 50% probability level using Johnson's ORTEP program.

The thermal parameters are not far from isotropic and of reasonable magnitude for low-melting organic crystals. For the most part rms thermal amplitudes vary between 0.2 and 0.3 Å for both modifications. The largest amplitude in both cases is for nitrile nitrogen and is in a direction consistent with libration about the azo-carbon bond. The nitrile carbons have smaller displacements but in the same directions. Argay and Sasvári have found the thermal parameters of the $P2_1/c$ modification consistent with rigid body translation and

(15) Gy. Argay and K. Sasvári, *Acta Crystallogr., Sect. B*, **27**, 1851 (1971).

(16) D. S. Malament and J. M. McBride, *J. Amer. Chem. Soc.*, **92**, 4586 (1970).

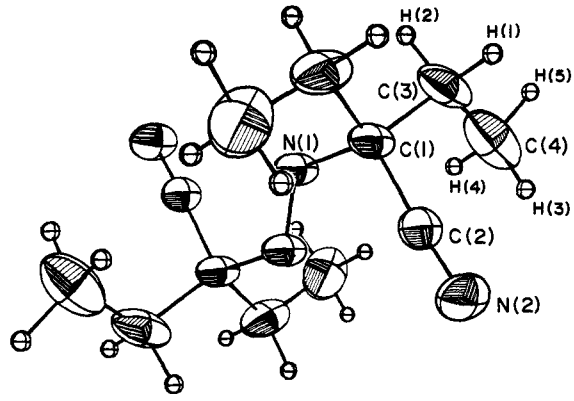

Figure 2. Molecular structure of the ordered model for ACP viewed from a point midway between the $-a$ and c axes with b vertical. The numbering of a part of the near half of the molecule corresponds to the scheme of Table VI. Thermal ellipsoids are drawn at the 22% probability level using Johnson's ORTEP program.

libration. Our parameters are roughly proportional to theirs and some 15–40% larger.

ACP. The ordered model for disordered ACP is illustrated in Figure 2. Bond lengths, angles, and torsional angles for this model (Table VIII) are remarkably similar to those of the other azonitriles. The only features of the model which reflect the disorder are a 1.50 Å C–C distance and a 116° C–C–C angle in the side chain and the unrealistic thermal parameters of all atoms (Table VII).

It is interesting that this model shows the same distortion of the nitrile nitrogen away from the azo grouping as do the AIBN models. In light of the expectation of reduced intermolecular dipolar interaction in ACP as compared to AIBN (see below), one can speculate that this distortion is due to intramolecular influences, perhaps to electrostatic repulsion by the azo group. The corresponding azo attraction for the nitrile carbon must be one factor favoring the eclipsed conformation for the azonitriles. The C—C≡N bond angle is 179.3° in muconodinitrile which has a similar packing but lacks the azo group.[17]

Crystal Packing. The most striking feature of the packing of these crystals is the arrangement of the nearly planar S-shaped backbones described above onto sheets which extend through the crystal in a manner analogous to that found for other dinitriles such as muconodinitrile[17] and dicyanoacetylene.[18] As shown in Table IX deviations from these sheets are as small for the backbone atoms in these crystals as for those in muconodinitrile (0.27 Å), but the spacing between sheets is of course greater (muconodinitrile, 3.257 Å) because of branching in the azo compounds. The left frames of Figure 3 show the arrangement of backbone atoms on the sheets. Within the sheets are vertical chains of translationally related molecules. The structures differ in spacing along the chain and in phase of rotation of the molecules about an axis perpendicular to the sheet as indicated by the nitrile chain angles in Table IX.

Adjacent chains in $P2_1/c$ and *Cmca* are related by screw axes to give the familiar herringbone pattern of

(17) S. E. Filippakis, L. Leiserowitz, and G. M. J. Schmidt, *J. Chem. Soc. B*, 305 (1967).
(18) R. B. Hannan and R. L. Collin, *Acta Crystallogr.*, 6, 350 (1953).

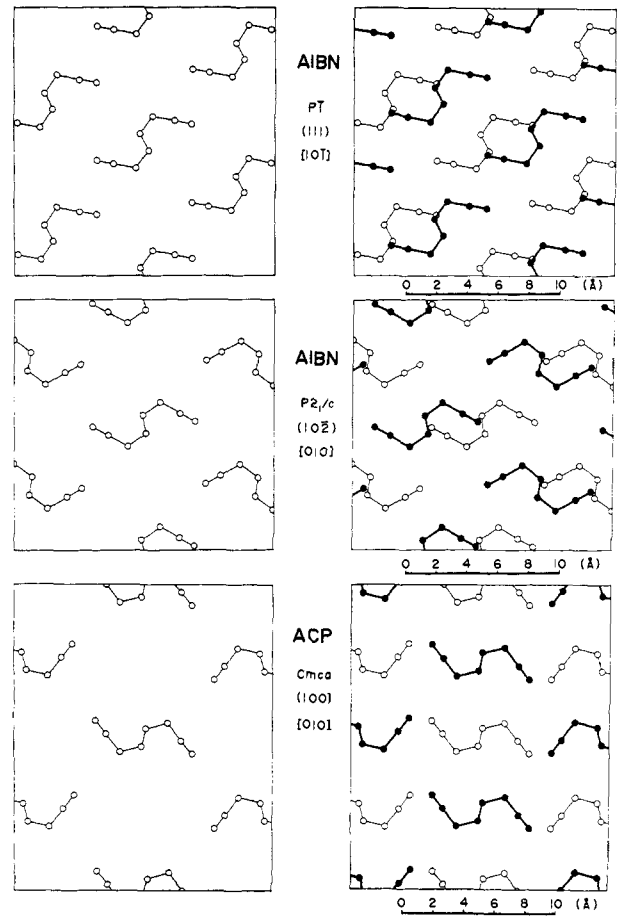

Figure 3. Azonitrile packings viewed along normal to the plane of N≡CCN=NCC≡N backbones with side chains omitted. Left frame shows a single plane; right frame shows the same plane with the next plane toward the viewer superimposed and darkened. Between frames are given compound, space group, plane of the page, and vertical direction in the page.

Table IX. Crystal Packing Parameters

	AIBN-d_{12} $P\bar{1}$	AIBN $P2_1/c$	ACP *Cmca*[a]
Sheet plane	(111)	(10$\bar{2}$)	(100)
Max deviation from sheet, Å	0.30	0.135	0[b]
Spacing between sheets, Å	4.444	4.113	4.529
Chain direction	[10$\bar{1}$]	[010]	[010]
Spacing along chain, Å	8.935	8.224	9.966
Nitrile chain angle, deg	81	60	37
Spacing between chains, Å	6.255	7.404	7.779
Nitrile–nitrile angle,[c] deg	180[b]	120	74

[a] From refinement of the disordered structure as if it were ordered. [b] Fixed by symmetry in this space group. [c] Angle between nitriles on adjacent chains.

nitrile groups observed in muconodinitrile and dicyanoacetylene. The angle between nitriles of adjacent chains is given in the table. The $P\bar{1}$ structure is related to the $P2_1/c$ by 180° rotation of the molecules of alternate chains about a horizontal axis in the page to give chains which are related by translation and are more closely spaced but maintain an antiparallel, herringbone-like pattern of nitrile groups. In light of this relationship it is tempting to speculate about a topotactic mechanism for the $P2_1/c \rightarrow P\bar{1}$ phase transformation at 70–80°,[1a] but there is no consistent relationship between

parent and daughter lattices, and even epitaxial growth of the $P\bar{1}$ phase is questionable.

The right frames of Figure 3 show the projection of the next sheet closer to the reader on the sheet shown in the left frames. In their Figure 3a Argay and Sasvári present a top view of the $P2_1/c$ packing.[15]

Chemical Implications. On the basis of the observed crystal packings one can confidently dismiss the hypothesis that KI formation from a radical pair in the crystal cage is suppressed by van der Waals interactions which prevent the nitrile nitrogen of one radical from approaching the trivalent carbon of the other. Examination of the left column of Figure 3 shows that if in approaching the geminate radical a nitrile group were to pivot about an axis perpendicular to the page through the trivalent carbon to which it is bound, it would come no closer than 3.5 Å to the nitrile nitrogen of a molecule in the adjacent chain. This distance is much greater than the sum of their van der Waals radii and is conservative, since the trivalent carbons themselves could separate once the covalent bonds to azo nitrogen are broken. Barriers imposed by passage between methyl groups of molecules on neighboring planes should also not be prohibitive. This is not visualized as readily from Figure 3, but a three dimensional model of the $P2_1/c$ packing shows paths in which the nitrile nitrogen–methyl carbon distance would always exceed 3.3 Å even with no cooperative motion of the trivalent carbon fulcrum.

On the other hand such motion of the nitrile group would radically alter the arrangement of dipoles in the crystal. The herringbone packing of nitrile groups is well-suited for optimizing the dipole–dipole attraction between molecules. Both pivoting of the free radical nitrile group about an axis perpendicular to the plane of Figure 3 to allow KI formation and approach of the trivalent carbons to form TMSN would oppose the dipolar forces exerted on the nitrile groups by their neighbors within the sheet.[19] Since pivoting about the axis of the nitrile group to bring a methyl group of the radical into position for hydrogen atom transfer to the geminate radical would not be opposed by these dipolar forces, the forces provide the basis for a qualitative rationalization for the predominance of disproportionation in photolysis of crystalline AIBN. The production of ketenimine from ACP could be rationalized in terms of the greater separation of the dipoles in this crystal.

Such a naive analysis cannot weigh properly the many factors determining the relative ease of various motions of the radical pair within its crystalline cage. For example, it ignores the potentially crucial role of the nitrogen molecule generated between the radicals. It seems likely that the only method of obtaining a sound qualitative appreciation for the importance of the factors governing the behavior of reactive organic intermediates in crystalline solids is by use of a digital computer. We have studied some aspects of the AIBN problem using empirical atom-pair potentials in an iterative program to simulate the motion of the cyanoisopropyl radical pair and nitrogen molecule in their crystalline environment. Since reliable pairwise potentials are not available for all the atoms involved in this problem, we have attempted to fix on a reasonable set by requiring that it predict energy minima for the observed crystal packings. Since sufficient data are not available for independent determination of all these parameters, we calculate the force along each of the coordinates which determine the observed packing[20] and the contribution from each parameter to each of the forces. Parameters are then adjusted manually to reduce the forces while keeping the parameters within reasonable limits. While this work is not yet complete, it is interesting to note that for our best current set of parameters the stabilization due to crystal packing is about two-thirds from polar interactions and only about one-third from van der Waals interactions. This observations underlines the qualitative importance of polar effects in determining the structure and reactivity patterns of organic crystals.

Isotope Effects. It is qualitatively clear from the data of Table I that the deuterated methyl group packs as if it were smaller than the unlabeled methyl, presumably for the most part because of differences in zero-point vibrational amplitude.[21] For the monoclinic modification this results in a shortening of each unit cell side by about 0.01 Å per molecule and a reduction of the cell volume by 0.3%. The size of this reduction is comparable to that found for solid methane[4] and calculated from theory for reduction of zero-point vibrational amplitude.[21] For the triclinic modification the differences are more erratic, and the volume reduction on deuteration is only 0.2%. Only three of the fractional coordinates change by as much as three standard deviations between deuterated and unlabeled $P\bar{1}$ structures. The most substantial change is in the x coordinate of the central carbon, C(1), which seems an unlikely result of deuteration. Hopefully the computer packing analysis mentioned above will allow us better to assess the subtle differences in packing between labeled and unlabeled compounds.

Acknowledgments. We thank the National Institutes of Health and the National Science Foundation for support of this work under Grants GM-15166 and GP-14607, respectively, and the NSF for a departmental instrument grant which allowed purchase of the diffraction equipment. Preliminary measurements were made using equipment of Professor H. W. Wyckoff, whom we thank for his hospitality and help.

(19) Nitrile groups in adjacent sheets are much less influential on this type of motion because of an unfavorable geometry.

(20) For example, in the monoclinic system the coordinates are a, b, c, β, and the three Eulerian angles orienting the molecule about a center of symmetry.

(21) (a) A. R. Ubbelohde, *Trans. Faraday Soc.*, 32, 525 (1935); (b) L. S. Bartell, *J. Amer. Chem. Soc.*, 83, 3567 (1961).